Nuclear Materials and Energy 27 (2021) 100952

Contents lists available at ScienceDirect

Nuclear Materials and Energy

journal homepage: www.elsevier.com/locate/nme

Development of DTT single null divertor scenario

L. Balbinot [a,b,*], G. Rubino [c], P. Innocente [b]

[a] Università degli Studi di Padova, Via VIII Febbraio, 35122 Padova, Italy
[b] Consorzio RFX, Corso Stati Uniti 4, 35127 Padova, Italy
[c] Centro Ricerche Energia, Ass. EURATOM-ENEA-CNR, CP 65 Frascati, Italy

ARTICLE INFO

Keywords:
DTT
Soledge2D-Eirene
Divertor
Scrape-off layer
Detachment

ABSTRACT

This paper focuses on scrape-off layer and divertor modelling of the medium-density single-null scenario of the Divertor Test Tokamak facility (DTT), under construction in Italy. The modelling was performed using the 2D coupled fluid-Monte Carlo code SOLEDGE2D-EIRENE. For DTT pump designing, neutral pressure at the pump aperture below the dome is calculated in deuterium-only cases as well as with impurity seeding with various puffing levels. This scenario analysis also allowed the characterization of detachment in DTT and the influence of pumping on detachment itself. Two different radiating impurities, neon and nitrogen, were tested in the high power scenario to evaluate the minimum impurity concentration required to achieve sustainable conditions at DTT divertor. The sensitivity of the model was studied by varying the impurity concentration; the model shows a hysteresis-like behaviour between the impurity influx and the total impurity content by which detachment is strongly influenced.

1. Introduction

Plasma exhaust to the divertor region is recognized by the EUROfusion roadmap [1] as one of the most critical issues to be solved towards the Demonstrative Fusion Power Plant (DEMO). The power loads predicted for next-generation machines pose extreme conditions to the plasma-facing components (PFCs) in the divertor region. The current technological limits for tungsten as PFCs require high radiated power fraction by impurities that may impact core performances. With current technological limits, the required radiative fraction in DEMO is about 90%.

Current experiments cannot operate with plasma parameters which are relevant to DEMO divertor designing such as P_{Tot}/R and SOL neutral opacity; alternative divertor solutions [2] must be tested in a DEMO-relevant environment. To bridge this gap, the Divertor Tokamak Test facility (DTT) is under construction in Italy. This machine will be able to partially match DEMO parameters such as P_{Tot}/R; thus DTT will have high field, high input power (up to 45 MW) and a relatively small mayor radius. The main goal of DTT is to test highly radiating alternative divertor solutions, such as Advanced Divertor Configurations (ADC) and liquid metal divertor, in DEMO relevant regimes [3].

This work describes the contribution to divertor plasma modelling and development of the conventional Single Null scenario in DTT. The modelling is performed with the edge numerical code SOLEDGE2D-EIRENE [4,5] that uses penalization technique [6] to extend plasma modelling to 2D obstacles, thus allowing a better description of plasma interaction with the entire first wall.

This modelling focuses on a single null scenario with 45 MW of input power, medium density ($n_{e,sep} = 8.0 \times 10^{19}$ m^{-3}, $n_e/n_G \simeq 0.7$) and is the most challenging scenario in terms of power handling. The main parameters used[1] in the scenario are in Table 1. Firstly, the modelling activity focuses on a power scan on deuterium-only cases under those conditions. Secondly it focuses on scrape-off layer (SOL) and plasma cooling optimization by comparing cooling efficiency of neon and nitrogen as seeded impurities and if the position of impurity puffing plays a role in determining divertor plasma conditions. The minimum impurity concentration to obtain sustainable heat flux to the divertor is calculated as well as the minimum radiated power fraction. This study also provides a prediction of neutral pressure in the sub-divertor region in various scenarios and under which conditions plasma load to the divertor are reduced to sustainable fluxes. Lastly, the dependency of the modelling results on initial conditions is analysed.

2. DTT single-null scenario

In its earlier stage DTT will be equipped with a full tungsten wall; the wall and divertor proposal are shown in Fig. 1a. Fig. 1b shows

* Corresponding author at: Consorzio RFX, Corso Stati Uniti 4, 35127 Padova, Italy.
E-mail addresses: luca.balbinot@igi.cnr.it (L. Balbinot), giulio.rubino@enea.it (G. Rubino), paolo.innocente@igi.cnr.it (P. Innocente).

[1] Some parameters, like minor and major axis, have been changed by few mm since the beginning of this work. It was decided to continue this work with the oldest parameters because such changes do not influence the scope and the results of this work.

https://doi.org/10.1016/j.nme.2021.100952
Received 31 July 2020; Received in revised form 11 January 2021; Accepted 16 February 2021
Available online 3 March 2021

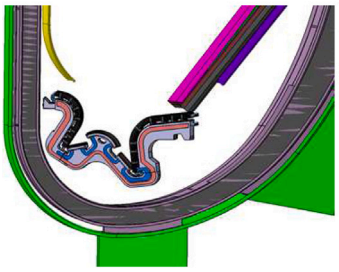

(a) Proposed divertor and sub-divertor region for DTT [7].

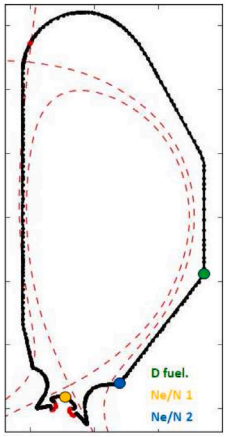

(b) First wall; dots represent puff. locations, abs. surfaces are red.

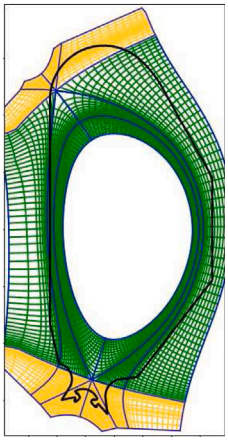

(c) Soledge2D grid; penalization technique extend it to the wall.

Fig. 1. DTT divertor and first wall poloidal view as in the project and as simulated.

Table 1
Main DTT parameters for the single null considered scenario as from the latest interim design report [7].

Parameter	Value
R	2.11 m
a	0.64 m
R/a	3.3
Volume	29 m^3
q_{95}	3
I_P	5.5 MA
B_T	6.0 T
H_{98}	1
P_{in}	45 MW
$n_{e,sep}$	8×10^{19} m^{-3}
λ_q	≃1 mm

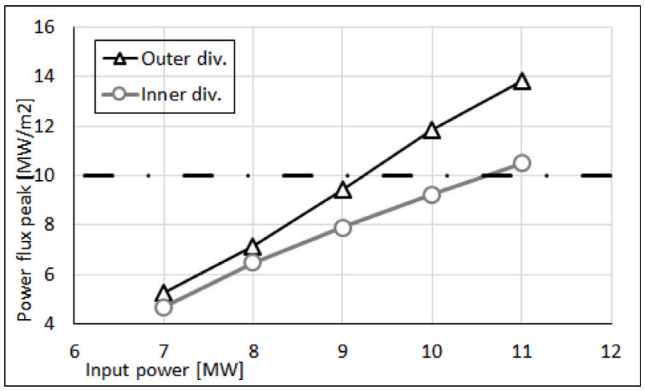

Fig. 2. Maximum power flux to the outer and inner divertor in the input energy scan of D-only simulations. The imbalance between inner and outer target is caused by the different connection length to the inner and outer divertor.

the first wall as simulated in SOLEDGE2D-EIRENE; total reflection of deuterium and impurities is set over the all wall (black lines) but on the absorbing surfaces (represented in red) that are the apertures that lead to the pump posed beyond the first wall. The albedo of the absorbing surfaces was set to match the target separatrix density; typical value is 0.92. When impurities are added, the albedo has been set equal to deuterium. Puffing locations are shown in Fig. 1b, deuterium fuelling is located near the low field side mid-plane while two different locations were tested for impurity seeding: the dome and the low field side of the external divertor plate.

According to [8] and plasma parameters in Table 1, the predicted cross-field heat flux decay length is: λ_q =1 mm, a narrow decay length given by the high field of the machine and comparable to the one predicted for ITER. The simple 2-point model [9] directly relates λ_q to the sum of heat diffusion coefficient for electrons and ions. By assuming λ_q =1 mm and $\chi_e = \chi_i = \chi$ the value for heat diffusion transport coefficient is set to χ =0.15 s/m^2. The particle diffusive transport coefficient was chosen as the typical value for ITER simulations: D =0.3 s/m^2. For this first scenario study, it has was chosen to keep all the transport parameters uniform over the all machine. Simulations are performed with no drift included.

Neutral species included in Eirene are atomic and molecular deuterium and impurities if seeding is inserted. In Soledge2D each ionization state of each impurity is treated as a single species; molecular deuterium ions are also included.

The scope of those simulations is determining the maximum amount of input power that can be transported from the core to the external wall, without exceeding the current maximum technological limit for tungsten divertor in steady-state conditions: 10 MW/m^2. They are also used as preliminary runs for seeded simulations. Puffing is set to 1.5×10^{22} D/s and albedo is adjusted to obtain the reference separatrix density: $n_{e,sep} = 8.0 \times 10^{19}$ m^{-3}. It was chosen to not use fixed albedo because one of the scope of this project was to assess the requirement for divertor pumping, in doing so, using different pumping regimes is preferable; the same choice was made in the runs described in Section 3.

Fig. 2 show the results of the input power scan. Results show the typical imbalance between inner and outer divertor power load, the latter always presenting higher power flux. For this reason, in this work it will be referred to attached or detached conditions referring to outer divertor plasma. Approximatively 9 MW is the maximum input power that provides sustainable conditions at the outer divertor thus implying that, in the 45 MW reference scenario, the minimum radiated power is about 36 MW, corresponding to a radiated fraction of 80%, confirming that this scenario can operate only in high radiation regimes.

3. Impurity seeding simulations and detachment thresholds

Nitrogen and neon have been tested as seeded impurities in the 45 MW scenario. Since SOLEDGE2D-EIRENE mesh is extended only few

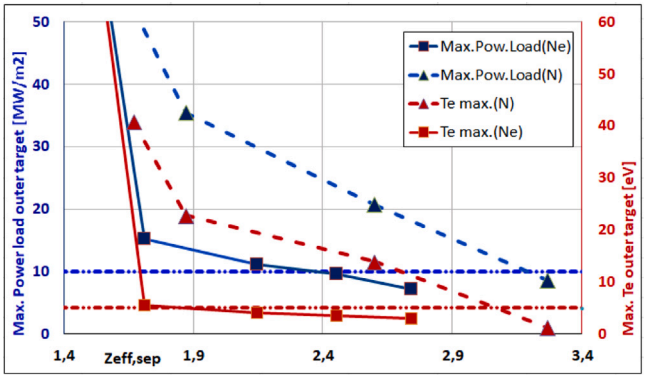

Fig. 3. Maximum power deposit to and maximum electron temperature at the outer target in simulations using nitrogen or neon as seeded impurity.

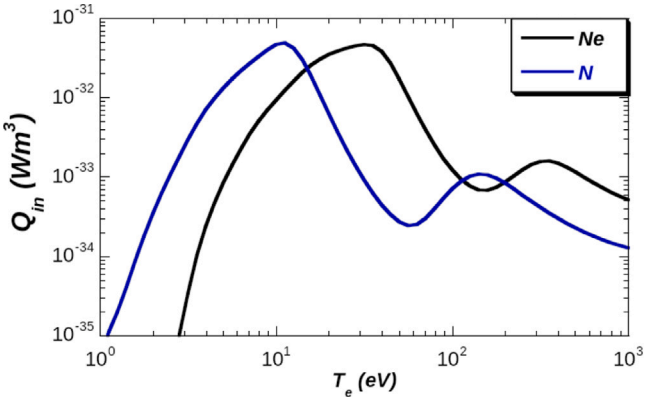

Fig. 4. Cooling rates by different impurities as function of electron temperature; curves are calculated by using rate coefficients from coronal equilibrium of atomic reactions in ADAS database [10].

cm inside the separatrix, the input power was set to 36 MW, assuming 9 MW radiated in the core. Deuterium puffing was kept constant ($\Gamma_D = 6.0 \times 10^{22}$ D/s) while neon and nitrogen puffing level were varied to compare Ne and N radiative cooling. Absorbing surface albedo was varied to match the scenario $n_{e,sep}$.

Fig. 3 shows the maximum power deposit to the outer target and the maximum temperature at the outer target in N and Ne cases. Results show that a certain degree of detachment can be achieved.[2] Fig. 3 shows that sustainable conditions at the outer divertor can be obtained with reasonable Z_{eff}, but also that with neon seeding lower Z_{eff} is needed due to its higher cooling rate at high temperatures, see Fig. 4. With nitrogen seeding, lower temperature can be achieved due to its higher cooling rate at low temperature. The difference between neon and nitrogen performances is even larger when considering a fixed P_{aux}, in that case $P_{In,N} > P_{In,Ne}$ since neon radiates more in the core; the same P_{In} was used in this study to avoid any further assumption. Higher radiated power fraction are radiated in neon cases than nitrogen cases, similarly to what was found in recent modelling on ASDEX-upgrade and ITER [12].

Neutral pressure at the two main pumping system entrances present similar behaviours in all the above mention cases and do not depend on the seeded impurity but on detachment level only, better description will be given in the next section. Plasma and neutral distribution in the private region in the attached and detached scenario is fundamental for pumping system design.

The total power flux to the wall includes the radiative contribution; it contributes from 40% of the power flux to the divertor with deep detachment, to be irrelevant when plasma attaches.

An attached and a detached case (the first and last point in Fig. 3) were also run with neon seeded from the secondary seeding location. The output showed no sensible difference in terms of radiated power, impurity penetration, or power deposition when compared to the previous simulations where seeding was done from the dome. No preferential puffing location was found.

4. Model sensitivity study

The sensitivity of the modelling and the dependence of the outcome on initial conditions were tested by slowly varying impurity influx. The albedo of the absorbing surfaces is fixed to 0.92 for each simulations for both D and Ne. Starting from the detached reference case: P_{in}=36 MW, $n_{e,sep} = 7.5\times10^{19}$ m^{-3}, $\Gamma_D = 6.0\times10^{22}$ D/s and $\Gamma_{Ne} = 1.5\times10^{21}$ Ne/s, see Fig. 5a; neon puffing is progressively reduced in various runs keeping constant all other parameters until complete attachment is reached at the outer target Fig. 5b with $\Gamma_{Ne} = 5.5 \times 10^{20}$ Ne/s. This study allows us to understand if attachment and re-detachment do follow the same path or not.

Results are shown in Fig. 6 where each point represent a run whose settings have been previously described. Attachment and re-detachment show a hysteresis-like behaviour: as shown in Fig. 6a, after attachment, much higher $\langle Z_{eff}\rangle_{sep}$ is needed to reduce the maximum power deposit to the outer divertor below the maximum power load that will be sustainable in DTT; the cycled is closed when detachment is achieved again with higher Z_{eff}. It is possible to distinguish between a "cold branch" and a "hot branch" of the graph that are encountered when going from detachment to attachment and from attachment to detachment respectively. Similar behaviour has been previously observed with the 2D edge code U-EDGE [13] when simulating long leg divertor scenarios for ARC. In that case, impurity concentration was calculated as a fixed fraction of main-plasma density.

With the decrease of neon influx, the radiated fraction of input power decreases and the power deposit to the outer target increases with the temperature in that region, for this reason, the neutral pressure at the entrance of the outer target pump entrance is reduced (Fig. 6d) so much that almost no neutral gas is pumped from that surface. This explains the increase of electron density shown by the blue line in 6b. The decrease of electron density at the separatrix does not follow the same path because the outer target keeps being attached at a higher neon puffing rate after plasma attaches; thus, pumping from the outer target region is slowed (red line in Fig. 6d). Electron density decreases only due to the increase of pumping efficiency at the inner target absorbing surface (red line in Fig. 6c).

There are two separate configurations: the first one in which neutrals are almost equally shared between inner and outer divertor, the second one in with after attachment, high temperatures compress neutrals to the inner divertor; the amplitude of DTT dome and the position of the strike points enhances this difference. The reason why this happens is explained in Figs. 7 and 8: neutral neon density, total neon density and total radiation due to neon are plotted in a attached and in a detached case respectively; the two outputs refer to simulations with the same neon input flux with the first being in the so-called hot branch and the second in the cold branch. In the attached case (7a), neutral neon particles moving to the outer divertor are immediately ionized, resulting in reduction of cross-field transport with respect to the transport of neutral species in 8a. Total neon density (Figs. 7b and 8b) is much lower in the attached case due to pressure conservation and the higher temperatures achieved in the attached case. Fig. 4 shows a decrease in neon cooling effectiveness with the increase of the temperature. The drop in cooling efficiency after detachment requires

[2] We do not discuss the most accurate definition of detachment or detachment degree [11]; in this case we refer to it has the sudden drop of temperature and power flux caused by impurity radiation as the one shown in Fig. 3.

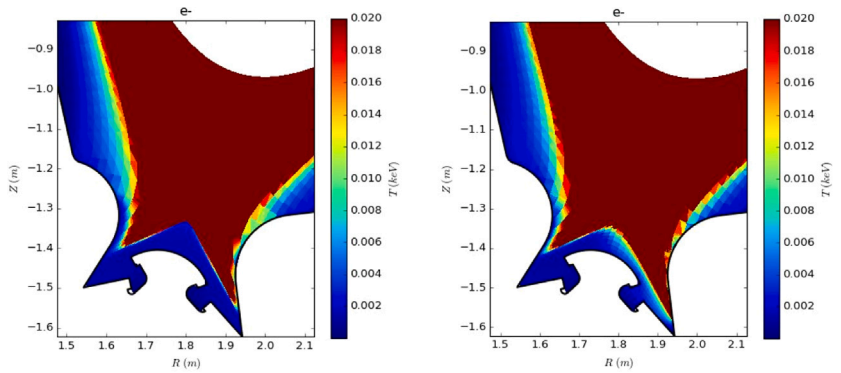

(a) Detached outer divertor case (b) Attached outer divertor case

Fig. 5. Electron temperature in divertor region saturated at 20 eV.

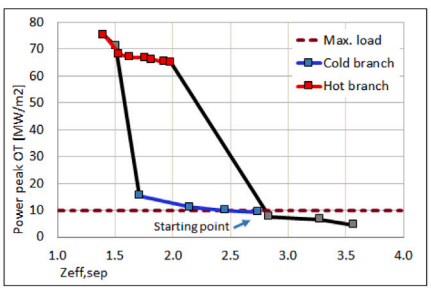

(a) Hysteresys-like behavior in seeded simulations.

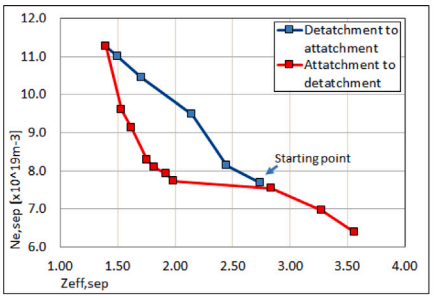

(b) $n_{e,sep}$ as function of Z_{eff} averaged on the separatrix.

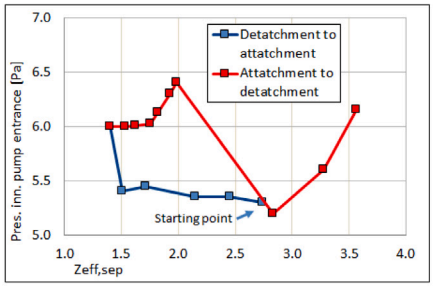

(c) Pressure at inner target absorbing surface.

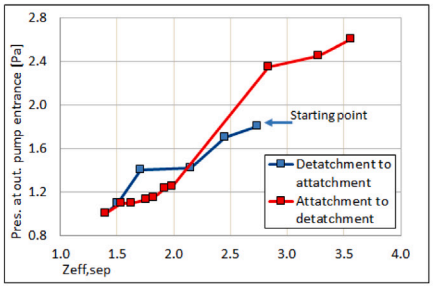

(d) Pressure at outer target absorbing surface.

Fig. 6. Hysteresis-like behaviour in seeded simulations. (For interpretation of the references to colour in this figure legend, the reader is referred to the web version of this article.)

higher quantity of impurity to re-detach the plasma and generates the hysteresis. The high neutral compression given by the geometry of the machine can play a role in limiting neutral transport and enhancing the hysteresis but further studies are needed.

It becomes evident that at least two different equilibrium can be achieved even with similar neon pressure: one with high temperature, low radiation, reduced transport and low neon density; the second is a high radiating, low temperature high neon density case.[3] It is reasonable to conclude that the re-arrangement of neutral particles after detachment or attachment persists and generates this hysteresis-like behaviour explained in this work.

[3] This statement does not affect the results presented in Section 3 because both seeding scans where made starting from a detached case.

5. Conclusions

Simulations of DTT maximum input power single-null scenario started from a deuterium only case and proceeded with impurity seeding. It was proven that this scenario can be operated obtaining sustainable power flux and temperature at both inner and outer divertor with both Ne and N seeding with acceptable $\langle Z_{eff} \rangle_{sep}$, with Ne providing better cooling efficiency and higher radiated power fraction. The variation of neutral pressure at the two main pump apertures is particularly important for pump designing, so it has been calculated with different degrees of detachment. This single-null analysis will be a benchmark for comparison of cooling performances with future alternative divertor modelling for DTT. Hysteresis-like behaviour was found when performing a scan on impurity flux amplitude, thus implying that attached or detached initial condition can influence the final divertor plasma conditions in terms of temperature and neutral pressure. In DTT

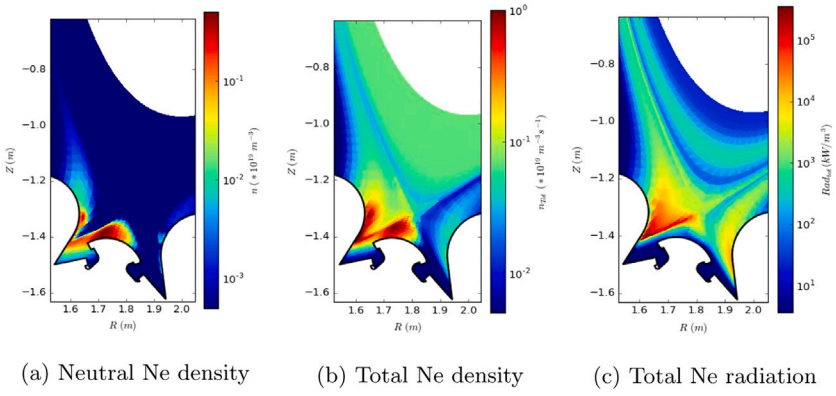

Fig. 7. Attached outer target scenario.

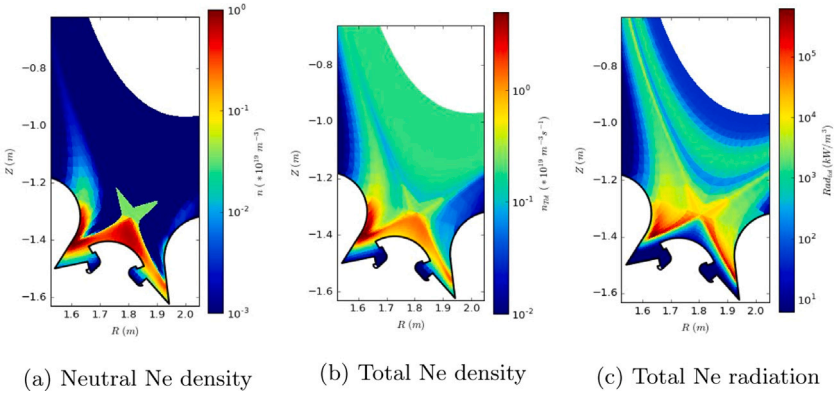

Fig. 8. Detached outer target scenario.

pre-existing divertor condition can determine if detachment is obtained with significantly higher or lower impurity content.

CRediT authorship contribution statement

L. Balbinot: Conceptualization, Methodology, Investigation, Writing - review & editing. **G. Rubino:** Investigation. **P. Innocente:** Conceptualization, Methodology.

Declaration of competing interest

The authors declare that they have no known competing financial interests or personal relationships that could have appeared to influence the work reported in this paper.

Acknowledgements

This work was performed within the 3nd cycle of MARCONI-FUSION HPC. The required computational resources were allocated under the project EM-CAD.
The work leading to this publication has been funded partially by Fusion for Energy (F4E). This publication reflects the views only of the authors, and F4E cannot be held responsible for any use which may be made of the information contained therein. The views and opinions expressed herein do not necessarily reflect those of the ITER organization. The authors have confirmed that any identifiable participants in this study have given their consent for publication.

References

[1] European Research Roadmap to the Realisation of Fusion Energy, Tech. rep..
[2] H. Reimerdes, et al., Assessment of alternative divertor configurations as an exhaust solution for DEMO, Nucl. Fusion 60 (6) http://dx.doi.org/10.1088/1741-4326/ab8a6a.
[3] G. Mazzitelli, et al., Role of Italian DTT in the power exhaust implementation strategy, Fusion Eng. Des. http://dx.doi.org/10.1016/j.fusengdes.2019.01.117.
[4] H. Bufferand, et al., Near wall plasma simulation using penalization technique with the transport code SOLEDGE2D-EIRENE, J. Nucl. Mater. 438 (SUPPL) http://dx.doi.org/10.1016/j.jnucmat.2013.01.090.
[5] H. Bufferand, et al., Numerical modelling for divertor design of the WEST device with a focus on plasma-wall interactions, Nucl. Fusion 55 (5) http://dx.doi.org/10.1088/0029-5515/55/5/053025.
[6] A. Paredes, et al., Penalization technique to model wall-component impact on heat and mass transport in the tokamak edge, J. Nucl. Mater. 438 (SUPPL) http://dx.doi.org/10.1016/j.jnucmat.2013.01.131.
[7] R. Martone, et al. (Eds.), DTT Divertor Tokamak Test Facility Interim Design Report: A Milestone Along the Roadmap To the Realisation of Fusion Energy, 2019.
[8] T. Eich, et al., Scaling of the tokamak near the scrape-off layer H-mode power width and implications for ITER, Nucl. Fusion 53 (9) http://dx.doi.org/10.1088/0029-5515/53/9/093031.
[9] V. Kotov, D. Reiter, Two-point analysis of the numerical modelling of detached divertor plasmas, Plasma Phys. Control. Fusion 51 (11) (2009) 115002, http://dx.doi.org/10.1088/0741-3335/51/11/115002.
[10] The-ADAS-Project, Open-adas database, https://open.adas.ac.uk/, version 2.1.
[11] R. Goldston, et al., A new scaling for divertor detachment, Plasma Phys. Control. Fusion 59 (5). http://dx.doi.org/10.1088/1361-6587/aa5e6e.
[12] E. Sytova, et al., Comparing N versus Ne as divertor radiators in ASDEX upgrade and ITER, Nucl. Mater. Energy 19 (2019) 72–78, http://dx.doi.org/10.1016/j.nme.2019.02.019.
[13] M. Wigram, et al., Performance assessment of long-legged tightly-baffled divertor geometries in the ARC reactor concept, Nucl. Fus. 59 (10) (2019) 106052, http://dx.doi.org/10.1088/1741-4326/ab394f.